Low-Divergent 940-nm Photonic-Crystal Surface-Emitting Laser for Short-Reach Free-Space Data Link

Chih-Hsien Cheng[1,#,*], Po-Lun Chen[2], Pin-Wei Ho[2], Yu-Heng Hong[3], Shih-Chen Chen[3], Shu-Wei Chang[4, 5], Chao-Hsin Wu[2], Hao-Chung Kuo[3, 5], Atsushi Matsumoto[1], Kouichi Akahane[1], and Gong-Ru Lin[2, 6,#,*]

[11]National Institute of Information and Communications Technology, Koganei, Tokyo 184-8795, Japan
[2]Graduate Institute of Photonics and Optoelectronics, and Department of Electrical Engineering National Taiwan University, Taipei 10617, Taiwan
[3]Semiconductor Research Center, Hon Hai Research Institute, Taipei 11492, Taiwan
[4]Research Center for Applied Sciences, Academia Sinica, Taipei 11529, Taiwan
[5]Department of Photonics and Institute of Electro-Optical Engineering, College of Electrical and Computer Engineering, National Yang Ming Chiao Tung University, Hsinchu 30010, Taiwan
[6]NTU-Tektronix Joint Research Center, Tektronix Inc. and National Taiwan University, Taipei 10617, Taiwan
[#]Equivalent Contributor and [*]Corresponding Author's e-mail: chcheng@nict.go.jp. grlin@ntu.edu.tw

Abstract: The photonic-crystal-structured surface-emitting laser with a low-divergent-beam angle of 4.5 mrad can perform either 5.5-Gbit/s NRZ-OOK, or 16-Gbit/s broadband QAM DMT or 19.2-Gbit/s bit-loaded DMT formats for 30-cm short-reach point-to-point free-space-optical communication link.

1. Introduction

Free-space optical (FSO) laser beam steering and communication is the future trend of wireless data link toward global broad-area network coverage without sacrificing the encoding bandwidth. In previous works, most of the visible and near-infrared wavelengths covering from 405 nm to 1550 nm have been explored for data communication. Among them, the 940-nm laser was one of the carriers within aforementioned bands seldom considered as the FSO carrier source for avoiding the signal-to-noise degradation on the eye-diagram of the received data stream after transmitting through the existed solar spectral background. Nevertheless, the 940-nm laser is suitable for enabling dual or multiple functionalities in versatile application fields such as light detection and ranging (LIDAR), low-earth-orbital satellite (LEOS) beacon, in-cabin automotive driver monitor and gesture recognition, and vehicle-to-vehicle (V-to-V) sensing, etc. [1-3], the large-mode-area and low-divergent-angle laser source has already emerged to play important roles for various users. Particularly for serving as the beacon or data carrier between satellites, the divergent angle of the laser beam is usually controlled in mrad or μrad regime. Therefore, The one-dimensional metallic/dielectric surface grating ot surface photonic crystal configuration is essentially the key to perform the low divergent beam within a wide lasing area of a semiconductor laser diode, which allows the steerable and/or structurable light field of the high-power laser beam maintained within the illuminating spot during distant propagation. One intriguing design is the photonic-crystal-structured surface-emitting laser (PhCSEL) which concurrently fulfills the demands of high power, large area, and low divergence for distant sensing and linking applications. To convey the possibility that the 940-nm laser carrier can also be a full compatible and supplementary candidate for short-reach data transmission when heterogeneously integrating with other microwave wireless network links, the parametric optimization on direct modulation bandwidth, the typical and advanced data formats with allowable encoding Baud rate, the short-reach networking performances of such a large-emission-area and low-divergent-angle PhCSEL are characterized in detail.

2. Experimental setup

In this experiment, the 940-nm TO-can-packaged PhCSEL with a rated power of 200 mW was available as a transmitter of the short-reach FSO data link, as shown in Fig. 1(a). In addition, the homemade-specific SMA package was employed to optimize the resistance-inductance-capacitance circuit of the 940-nm TO-can-packaged PhCSEL transmitter for improving the transmission bandwidth, as shown in Fig. 1(b). The testing transmission system of the short-reach FSO data link is illustrated in Fig. 1(c). Before the transmission, the MATLAB software generated the non-return-to-zero on-off keying (NRZ-OOK), broadband quadrature amplitude modulation discrete multitone (QAM DMT), and bit-loaded DMT data streams. Then, the generated NRZ-OOK, QAM-OFDM, and bit-loaded DMT data streams were sent to an arbitrary waveform generator (AWG) with a sampling rate of 64 GSa/s and an analog bandwidth of 25 GHz for the electrical signal generation. The NRZ-OOK, QAM-OFDM, and bit-loaded DMT data streams with an original peak-to-peak voltage of 300 mV were amplified via a 21-dB microwave amplifier. A bias-tee with an analog bandwidth of 6 GHz combined the direct-current (DC) bias and the data stream to drive the 940-nm PhCSEL. The distance of the short-reach FSO data link was set as 0.3 m. At the received end, the 7-GHz ultrafast photodiode (UPD) was used to receive the transmitted QAM OFDM data stream. After the optical-to-electrical conversion, the post microwave amplifier with an analog bandwidth of 10 GHz was utilized to amplify the converted data stream. Finally, the mixed-signal oscilloscope (MSO) captured the amplified data stream to analyze the transmission performances such as the error vector magnitude (EVM), the signal-to-noise ratio (SNR), and the bit-error-ratio (BER).

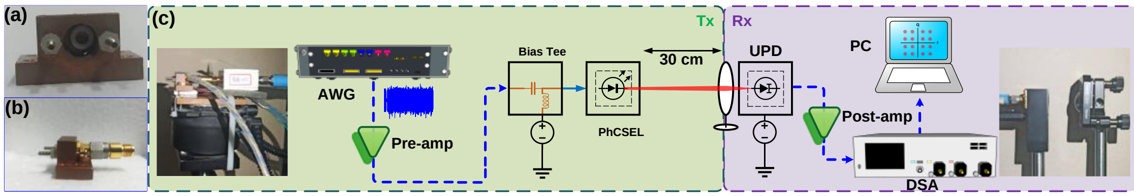

Fig. 1. (a) Photograph of the 940-nm PhCSEL; (b) Photograph of the laser package; (c) Photograph and schematic diagram of the testing transmission system of the short-reach FSO data link.

3. Results and discussions

Figure 2(a) shows the power-to-current (*P-I*) and voltage-to-current (*V-I*) curves of the 940-nm PhCSEL. From the *P-I* curve, the threshold current (I_{th}) of the device is measured as 213 mA. In addition, the slope efficiency of the 940-nm PhCSEL can be obtained as 0.26 W/A and a differential quantum efficiency of 34.3%. With the photonic crystal structure, the 940-nm PhCSEL exhibits linear modulation when the device is operated above the threshold current. From the *V-I* curve, the differential resistance of the 940-nm PhCSEL is acquired as 4.5 Ω beyond the threshold current. The reflection coefficient of this 940-nm PhCSEL is evaluated as 0.83 from the differential resistance. Furthermore, the return loss and voltage standing wave ratio can be estimated as 1.62 dB and 10.8 when the 940-nm PhCSEL is operated at $2I_{th}$ (426 mA). From the abovementioned results, the strong signal reflection during the direct modulation induces the requirement of a larger amplitude for the signal injection.

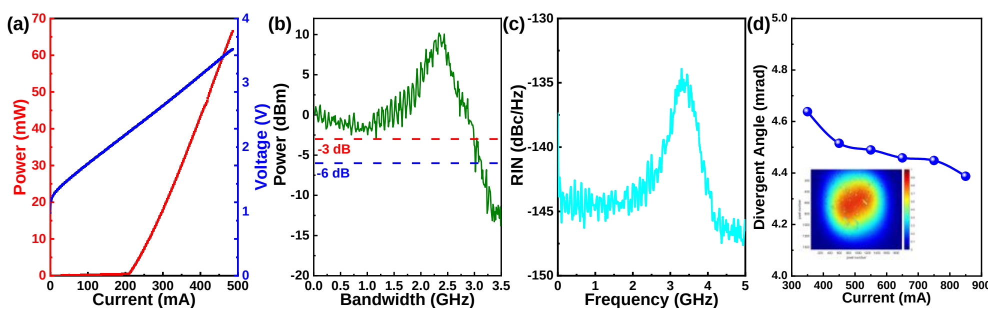

Fig. 2. (a) The *P-I* and *V-I* curves of the 940-nm PhCSEL operated under different DC biases; (b) the frequency response and (c) the RIN spectrum of the 940-nm PhCSEL operated under the $2I_{th}$ condition; (d) the divergent angle of the 940-nm PhCSEL operated under different DC biases.

In addition, the small signal response of the 940-nm PhCSEL operated at the $2I_{th}$ condition is illustrated in Fig. 2(b). By operating at $2I_{th}$, the 940-nm PhCSEL exhibits its 3- and 6-dB bandwidths of 2.98 GHz and 3.13 GHz. The relaxation oscillation frequency of this 940-nm PhCSEL can also be observed at 2.35 GHz. To avoid the noise figure of the 940-nm PhCSEL on decaying the SNR of the transmitted data stream, the relaxation intensity noise (RIN) response of the 940-nm PhCSEL is analyzed in Fig. 2(c). Under the $2I_{th}$ operation, the peak frequency and peak power of the relaxation oscillation-related RIN frequency are respectively obtained as 3.3 GHz and -135 dBc/Hz. The RIN of the 940-nm PhCSEL can be suppressed by increasing the bias current to improve its noise figure performance and modulation bandwidth for facilitating the high-quality data encoding result. To observe this 940-nm PhCSEL applying as a transmitter of the short-reach FSO data link, the experiment related to the divergent angle needs to perform. Figure 2(d) shows the divergent angle of the 940-nm PhCSEL operated under different DC biases. When the DC bias increases from 350 mA to 850 mA, the divergent angle of the 940-nm PhCSEL decreases from 4.6 mrad to 4.3 mrad. Detuning the DC bias current between 350 mA and 850 mA only contributes to the maximal variation of 3.3%. This divergent angle of the 940-nm PhCSEL corresponds to the divergent angle regime of the short-reach FSO data link.

For the short-reach FSO data transmission, the receiving eye-diagrams of the NRZ-OOK data at 5 and 5.5 Gbit/s without the digital signal processing (DSP) compensation are compared in Fig. 3(a). In Fig. 3(a), the 940-nm PhCSEL can deliver the 5-Gbit/s NRZ-OOK data to achieve error-free BER ($<10^{-9}$) of 4.6×10^{-12} qualified for the datacom standard. In more detail, the 5-Gbit/s NRZ-OOK data stream provides a receiving amplitude of 117.8 mV with a corresponding SNR of 16.65 dB and rising/falling time of 106.7/105.6 ps. By increasing the data rate to 5.5 Gbit/s, the amplitude and SNR degrade to 91.9 mV and 14.8 dB. The corresponding BER degrades to 1.8×10^{-9} close to the datacom standard. To increase the bandwidth usage of the 940-nm PhCSEL, the broadband 16-QAM DMT data format is utilized. Figure 3(b) shows the SNR spectrum and the constellation plot of the 4-GHz 16-QAM DMT data stream carried by the 940-nm PhCSEL. For this transmission test, the operated DC bias is set as $2I_{th}$ to avoid waveform distortion. In Fig. 3(b), the constellation plot of the received data stream reveals an EVM of 15.3% to obtain the average SNR of 16.3 dB. In addition, the corresponding BER is evaluated as 1.3×10^{-3} to pass the forward error correction (FEC) standard with a BER of 3×10^{-8}. From the abovementioned results, the 940-nm PhCSEL can transmit the 4-GHz 4-QAM OFDM data stream with a corresponding data rate of 16 Gbit/s.

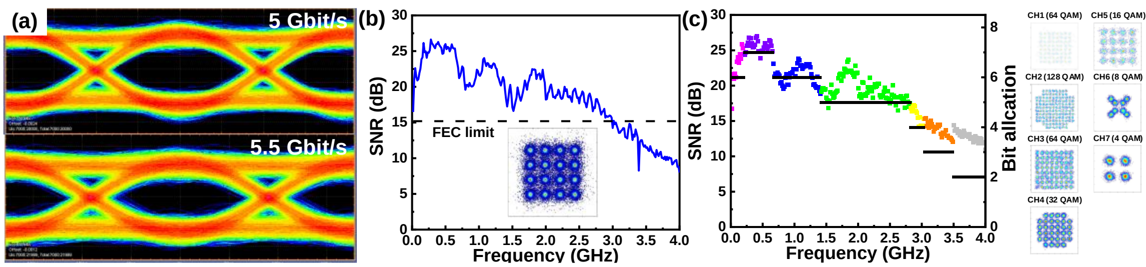

Fig. 3. (a) Eye-diagrams of the 5-Gbit/s and 5.5 Gbit/s NRZ-OOK data streams transmitted by the 940-nm PhCSEL. (b) SNR spectrum and constellation plot of the 4-GHz 16-QAM DMT data stream transmitted by the 940-nm PhCSEL. (c) SNR spectrum and corresponding constellation plots of the bit-loaded DMT data stream transmitted by the 940-nm PhCSEL.

To maximize the data transmission capacity, the bit-loaded DMT data format is further used. The adaptive QAM mapping is used to distribute different bit levels according to the transmission characteristics for each subcarrier. Based on the SNR spectrum of the 16-QAM DMT data, the bit distributed in subcarriers by the self-adaptive algorithm can slightly change the allocation strategy by adjusting the limitation between different QAM levels. The whole SNR spectrum is divided into 7 channels to distribute different QAM levels. For the channels 1-7, the QAM levels are individually set as 64-QAM/128-QAM/64-QAM/32-QAM/16-QAM/8-QAM/4-QAM with corresponding allowable bit-loaded bandwidths of 0.2 GHz/0.45 GHz/0.75 GHz/1.41 GHz/0.22 GHz/0.45 GHz/0.52 GHz. As a result, the receiving SNRs of the bit-loaded DMT data are respectively obtained as 21.4 dB/25.0 dB/21.0 dB/18.8 dB/15.1 dB/13.1 dB/11.8 dB for 64-QAM/128-QAM/64-QAM/32-QAM/16-QAM/8-QAM/4-QAM to support the total allowable data rate of 19.18 Gbit/s. From the abovementioned discussion, this 940-nm PhCSEL can be regarded as one of the candidates for the short-reach FSO transmitter.

4. Conclusion

With the 940-nm PhCSEL with a low-divergent-beam angle of 4.5 mrad, the 19.2-Gbit/s bit-loaded DMT transmission over 30 cm is demonstrated for short-reach point-to-point FSO data link. With the -3-dB analog bandwidth of 2.98 GHz, the 5.5-GHz NRZ-OOK data can be successfully transmitted with a corresponding SNR and BER of 14.8 dB and 1.8×10^{-9}. To effectively increase the bandwidth usage of the device, the PCSEL can deliver the 16-Gbit/s 16-QAM DMT data with an EVM of 15.3%, an SNR of 16.3 dB, and a BER of 1.3×10^{-3} to pass the FEC criterion. By the self-adaptive algorithm to perform the QAM mapping, the bit-loaded DMT data stream with a corresponding data rate of 19.18 Gbit/s is demonstrated. Besides the light detection and ranging (LiDAR) application, this 940-nm PhCSEL can be used as the short-reach FSO transmitter in the future.

5. References

[1] H. Liu, P. Miao, Y. Xiao, C. Liu, Z. Zhang, and J. Wang, "High performance multi-junction VCSELs for LiDAR applications," Proc. SPIE **12020**, 1202005 (2022).

[2] R. F. Carson, M. E. Warren, J. R. Joseph, T. Wilcox, D. J. Abell, and K. J. Otis, "Compact VCSEL-based laser array communications systems for improved data performance in satellites," Proc. SPIE 9226, 92260H (2014).

[3] J. Foresi, M. E. Warren, M. K. Block, L. Yang, K. Toledo, C. J. Helms, and G. Bacchin, "VCSEL arrays for quasi-continuous-wave applications," Proc. SPIE 10938, 109380D (2019).